

Shapes of Krill Swarms and Fish Schools Emerge as Aggregation Members Avoid Predators and Access Oxygen

Andrew S. Brierley^{1,*} and Martin J. Cox¹

¹Pelagic Ecology Research Group, Gatty Marine Laboratory, University of St Andrews, Fife KY16 8LB, Scotland, UK

Summary

Many types of animals exhibit aggregative behavior: birds flock, bees swarm, fish shoal, and ungulates herd [1]. Terrestrial and aerial aggregations can be observed directly, and photographic techniques have provided insights into the behaviors of animals in these environments [2] and data against which behavioral theory can be tested [3]. Underwater, however, limited visibility can hamper direct observation, and understanding of shoaling remains incomplete. We used multibeam sonar to observe three-dimensional structure of Antarctic krill shoals acoustically [4]. Shoal size and packing density varied greatly, but surface area:volume ratios (roughnesses) were distributed narrowly about $\sim 3.3 \text{ m}^{-1}$ [5]. Shoals of clupeid fish (e.g., sardine, anchovy) from geographically and oceanographically diverse locations have very similar roughnesses [6–8]. This common emergent shape property suggests common driving forces across diverse ecosystems. Group behavior can be complex [9], but a simple tradeoff—that we model—in which individual fish and krill juggle only their access to oxygen-replete water and exposure to predation can explain the observed shoal shape. Decreasing oxygen availability in a warming world ocean [10] may impact shoal structure: because structure affects catchability by predators and fishers [11–13], understanding the response will be necessary for ecological and commercial reasons.

Results and Discussion

We used multibeam sonar to survey for Antarctic krill (*Euphausia superba*) off the western Antarctic Peninsula [4, 5]. Krill aggregate into subsurface shoals in daylight (we use “shoal” generically here to mean pelagic aggregation: the terms “krill swarm” and “fish shoal” are in common use and sometimes imply random orientation of individuals; “school” usually applies to polarized aggregations of fish [14]), dispersing under cover of darkness to feed at night in the food-rich near-surface zone [15]. Shoals are fundamental units of organization for many pelagic species [11, 16], but sampling difficulties have left knowledge of shoal structure and of mechanisms of shoal formation in free-living populations incomplete. We detected 1084 krill shoals in daylight along 112 km of survey track through water between 17 m and 140 m deep over the course of a 5-day survey. One thousand and six shoals fell entirely within the sonar’s effective sampling volume, and we were able to obtain direct measures of three-dimensional (3D) size and shape for these shoals. Shoal length (x), width (y), vertical extent (z), and packing density were extremely variable (x range = 10–967 m, mean = 109 m, coefficient of variation

[CV] = 0.8; y range = 6–151 m, mean = 23 m, CV = 0.8; z range = 4–77 m, mean = 11 m, CV = 0.7; density range = <4 –804 individuals per m^3 , mean = 114 individuals per m^3 , CV = 0.8), but 3D shape, as described by the surface area:volume ratio, or roughness (R), was distributed narrowly about a mean of 3.3 m^{-1} (range 1.2 m^{-1} to 8.2 m^{-1} , CV = 0.2) (Figure 1; Figure 2A).

The shape $R \sim 3.3 \text{ m}^{-1}$ does not approximate to any familiar geometric shape such as a sphere, ellipsoid, or cylinder. Fish schools have been described as amoeboid [7, 17], but, because of the apparent surface angularity, we prefer to describe the shape of krill shoals we observed as a multifaceted lozenge (see Figure S1 available online). Furthermore, whereas R for observed krill shoals was consistent for shoals spanning a large range of sizes (R was determined from the slope of the statistically significant linear fit of surface area against volume over all shoals [5], coefficient of determination = 0.97, $p < 2.2 \times 10^{-16}$; see Figure 1), R for geometric shapes varies with total size.

There are three published studies reporting shoal roughness of wild marine fish [6–8]. These studies used multibeam sonar to survey four species of clupeid (*Sardinops sagax*, *Sardinella aurita*, *Engraulis ringens*, and *Strangomera bentincki*) in temperate and tropical regions of the Atlantic and Pacific oceans. Shoals of all species were highly variable in density and x, y, and z dimensions but also had $R \sim 3.3 \text{ m}^{-1}$ (weighted mean of all shoals 3.6 m^{-1} , range of means 3.0 m^{-1} to 5.7 m^{-1}) (Figure 1). The similarity of $R \sim 3.3 \text{ m}^{-1}$ for shoals of fish and krill is remarkable, and all data together reveal a previously unrecognized cross-taxa isometric scaling. The common emergent property $R \sim 3.3 \text{ m}^{-1}$ suggests that common driving forces influence the shape of pelagic aggregations of taxonomically and physiologically diverse organisms across diverse ecosystems. Krill and fish also form “layers” [6, 18], and “thin” layers are recognized as ecologically important entities [19]. Gerlotto et al. [6] have reported an R of 6.4 m^{-1} for layers of clupeid fish. Layers may be more common at night, when visual predation is reduced [20] and the stimulus for prey to aggregate in to shoals is diminished; our krill surveys were conducted in daylight. Furthermore, because they are so extensive, layers can be thought of as 2D rather than 3D features; for these reasons, we do not consider layers any further in subsequent analysis.

What are the common driving forces that lead to a common shoal shape of $R \sim 3.3 \text{ m}^{-1}$? Numerous physical and biological drivers for animals to aggregate have been proposed [1]. However, the two most basic short-term objectives of any animal (within the limits of their physiological tolerances) are (1) to obtain sufficient oxygen to satisfy metabolic demands and (2) to avoid being eaten. Longer-term goals include food acquisition and reproduction, but individuals that fail in the former two objectives cannot achieve these. In his classic paper “Geometry for the selfish herd,” Hamilton [21] argued that terrestrial animals would strive to maintain a position toward the middle of an aggregation because this would provide protection from predators attacking from the edge. The concept of selfish herd behavior is relevant in a pelagic context [22], but in the pelagic environment, the challenge for individuals expands from two dimensions to three because

*Correspondence: asb4@st-and.ac.uk

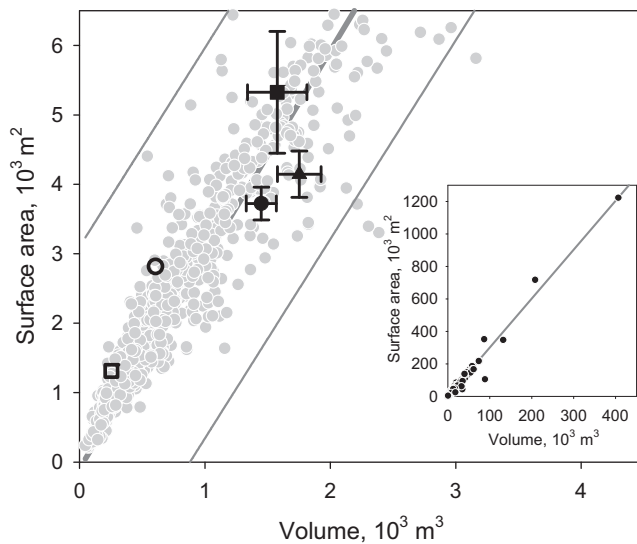


Figure 1. Surface Area:Volume Relationships for Shoals of Antarctic Krill and Clupeid Fish

Inset: values for all 1006 observed individual krill shoals, and the highly significant linear regression ($p < 2.2 \times 10^{-16}$; solid gray line) showing that surface area:volume (roughness) remains constant over the entire range of shoal sizes. Main panel: a truncated krill data set over a size range conducive to comparison with fish. (Fish shoals were observed in shallower water than krill and, because of simple space constraints, shallow water cannot accommodate such large aggregations as deep water. As a consequence, fish shoals had a smaller range of dimensions than krill shoals.) \blacktriangle , *Sardinops sagax* off Mexico [8] with standard errors (SE) ($n = 257$); \blacksquare , *Sardinella aurita* off Senegal [8] with SE ($n = 68$); \bullet , *S. aurita* off Venezuela [8] with SE ($n = 343$); \circ and \square , *Engraulis ringens* and *Strangomera bentincki* off Chile [6] (these fish were in single-species shoals but were separated by shoal type, not species [6]; \circ = mean for 261 “schools” [length:height < 7], \square = mean for 154 “layers” [length:height > 7]).

shoals are 3D structures that can be attacked from above and below as well as from the sides. Multibeam sonar enables the examination of this third dimension [23]. If predation were the only force driving shoal shape, a sphere would be the optimal shape because that would provide the smallest surface area: volume ratio and would enable the largest possible proportion of individuals to occupy internal, sheltered positions away from the edge. Shoals of krill and fish were clearly not spherical, so we investigated whether the apparently conserved emergent shoal property of $R \sim 3.3 \text{ m}^{-1}$ could be explained simply in terms of a tradeoff by individual shoal members between predator avoidance and oxygen acquisition.

We hypothesized that, in line with Hamilton [21], individuals would favor an interior position in a shoal because that would reduce the risk of predation: stragglers at the edge of fish shoals suffer greater predation mortality than individuals in the interior [24], and, although baleen whales consume entire krill shoals, most predation pressure upon krill is from predators that target individuals (Laws [25] indicates that whales consume <190 million metric tons of krill per year, whereas fish, squid, birds, and seals that prey on individual krill take 280 million metric tons per year). We further hypothesized that the time that individuals could remain within the protective confines of a shoal interior might be limited by oxygen availability. The rate of diffusion of oxygen through seawater is low, and even over very short distances, metabolic consumption of oxygen can exceed replacement by diffusion [26] (Figure 3). Fish shoals can deplete local

oxygen concentrations [27], and theoretical studies suggest that krill shoal size could be constrained by oxygen availability [28]. We used published information on oxygen consumption rates by krill and fish; empirical data on shoal dimensions (from multibeam sonar observations), animal size, and packing density; and dissolved oxygen concentrations and oxygen diffusion rates appropriate for temperatures at shoal locations to calculate the time it would take for oxygen concentrations in each observed shoal to be brought down by respiration to critical levels for each species (see Supplemental Experimental Procedures and Table S1). This oxygen depletion time is equivalent to the maximum time that an individual could remain at the center of the protective interior of a shoal before having to make an excursion to oxygen-replete but exposed (to predators) waters at the shoal’s edge. We determined the total number of animals in each shoal and calculated the number occupying positions at the edge. We then calculated a benefit factor, B , for each observed shoal, as

$$B = \frac{n_{\text{inside}} \times t_{\text{depletion}}}{n_{\text{total}}} \times \frac{n_{\text{edge}}}{n_{\text{max all shoals}}} \quad (\text{Equation 1})$$

where n_{inside} is the number of animals inside the shoal in question, $t_{\text{depletion}}$ is the time it would take for oxygen concentration at the center of the shoal to be brought down to the critical level for the species, n_{total} is the total number of animals in the shoal (i.e., numbers inside the shoal and on the shoal edge combined), n_{edge} is the number of animals on the shoal edge, and $n_{\text{max all shoals}}$ is the maximum total number of animals in any shoal of the species in the location under consideration. The higher the value of B (units = seconds), the longer the period of oxygen-unrestricted shelter the interior of a shoal can provide for an individual shoal member. The component of Equation 1 dividing the number of animals on the edge of the specific shoal in question by the number of animals on the edge of the largest observed shoal (for each species in each location of study) is included in accordance with the argument of Hamilton [21] that the bigger the group, the greater the chance that someone else will be eaten: thus, it is more beneficial for an individual to be in a large group than a small one.

We also calculated theoretical benefit factors for simulated shoals generated by packing the volumes of observed shoals in to a range of simple geometric shapes (sphere, cylinder, ellipsoid; see Supplemental Experimental Procedures) and more complex shapes that approximate some previously reported shoal shapes [11] (dumbbell, six- and eight-limbed sphere; Figure S2; Table S2). We manipulated the surface area:volume ratios (R) for these more complex shapes (see Supplemental Experimental Procedures) to explore theoretically the dependence of oxygen depletion time and exposure to predation on R , and thus the relationship between B and R . The graph of B against R (Figure 2B; see also Figure S3) shows B for simulated krill shoals peaking at $R \sim 3.3 \text{ m}^{-1}$. Benefit factors for observed shoals of krill and *Sardinella aurita* overlap the simulated krill shoal peak (Figure 2). $R \sim 3.3 \text{ m}^{-1}$ appears to provide the optimum combination of shelter from predation and accessibility to oxygen for pelagic crustaceans and fish in diverse ecosystems: to paraphrase Hamilton, we suggest that a tradeoff by individual shoal members between predator avoidance and oxygen acquisition shapes the selfish shoal.

Shoaling behavior and its response to various biological and physical stimuli has been monitored in tanks, but the limited

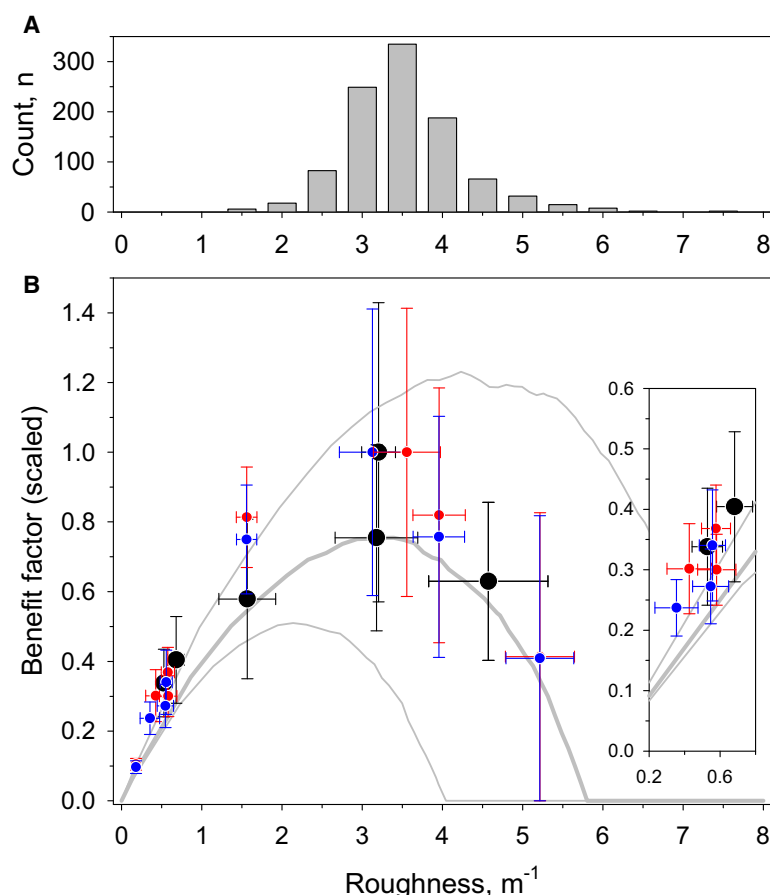


Figure 2. Roughness and Benefit Factor for Krill and *Sardinella* Shoals

(A) Distribution of observed roughness (R) for 1006 krill shoals (see Figure S1 for 3D visualizations of krill shoals). Shoals are dynamic features that form and disperse; the narrow spread in R about 3.3 m^{-1} could be due to observations capturing these dynamic processes.

(B) Variation in benefit factor (B) with roughness (a scaled B is used to facilitate display of fish and krill data on a common axis: scaled B for each species = B for a particular shoal/maximum B for all shoals of that species). The thick gray line is the median B for 1006 simulated krill shoals for which the observed krill shoal volumes were packed in to six-limbed spheres manipulated to have R between ~ 0 and 8 m^{-1} (see Figure S2 for schematic representations of shoal shape). Simulated shoals contain krill of mean observed size (length = 45.4 mm) swimming at a nominal speed of 20 cm/s (see Figure S3 for results from simulated shoals of large and small fast-swimming krill, results that reveal the same pattern of theoretical B peaking at $R \sim 3.3 \text{ m}^{-1}$). The thin gray lines are the observed 65th- and 35th-percentile ranges of the simulations. Black circles are median values for krill aggregations with observed volume packed, with increasing R , into a sphere, a cylinder, an ellipsoid, as observed, a dumbbell, and a six-limbed sphere. Blue and red circles are median values for 1000 simulated shoals of sardinella (*Sardinella aurita*) off Venezuela (blue) and Senegal (red) for which the simulated shoal volumes were packed, with increasing R , into spheres, ellipsoids, dumbbells, cylinders, six-limbed spheres, as observed, and two versions of eight-limbed spheres. Error bars are 65th- and 35th-percentile ranges. Inset: expanded view for $0.1 \leq R < 0.8 \text{ m}^{-1}$ and $0 \leq B$ (scaled) < 0.60 .

space and small numbers of individuals inherent with captive studies [24, 29] bring into question the extent to which these observations are representative of processes in the wild. Several experimental studies have investigated the impact of reduced oxygen concentrations on aggregations of captive fish. These studies have shown that aggregation dimensions increase, and that individual fish swim more rapidly and change position more frequently, as dissolved oxygen concentration declines [30, 31], but they have not been able to characterize the true 3D structure of shoals. Furthermore, as oxygen concentration is reduced experimentally in aquaria, the oxygen reduction impacts the entire water volume, and stressed fish have no higher-oxygen zone to escape to. Multiple studies have considered the interplay between hypoxia and antipredator behavior in fish [32, 33], and others have commented on the influence that oxygen availability may have on shoal shape and/or size [27, 34], but the present study is, to our knowledge, the first to develop a model framework with 3D field data and the first to expose common cross-taxa aggregation behavior.

Group behavior can be complex [9], but we have shown here that a simple mechanism, in which individuals within shoals juggle only their access to oxygen-rich water and exposure to predation, can explain observed shoal shape. Other factors, including self-pollution by excretion [28] and nearest neighbor distance [35] and attraction/repulsion [36], may well influence shoal shape, but the oxygen acquisition/predator avoidance framework we have developed here is one of the most parsimonious. A model using distance of individuals from the edge of the shoal, rather than oxygen depletion time, to

calculate benefit factor gave a maximum B at $R \sim 2.1 \text{ m}^{-1}$ and a distribution of B versus R that was significantly different from the distribution shown in Figure 2B (two-sample Kolmogorov-Smirnov test, $p = 0.005$). Distance of an individual to the nearest shoal edge gives a measure of how easy it would be for the individual to collect external resources of any kind, including food; the fact that such a model does not yield results that match observed data, whereas a model including an oxygen depletion component does, strengthens our argument that short-term oxygen demand plays an important role in driving shoal shape. A multibeam study of the internal morphology of shoals of freshwater fish revealed vacuoles inside shoals [37]. Our data-processing procedure did not enable us to identify vacuoles, but consideration of these and their potential role as reservoirs of oxygen could be a fruitful line for further investigation.

Krill swarms and clupeid shoals have a common emergent shape property characterized by $R \sim 3.3 \text{ m}^{-1}$. This shape provides individual aggregation members with an optimal tradeoff between predator avoidance and oxygen acquisition. Oxygen solubility in seawater is inversely proportional to temperature, and oxygen concentration in the world ocean has decreased since the 1950s [10], with further decreases likely as the world ocean continues to warm. We estimate that in the initial stages of future warming (through the region where the relationship between dissolved oxygen concentration and water temperature is essentially linear), oxygen depletion time will reduce by 3% for every 1°C of warming. To preserve $R \sim 3.3 \text{ m}^{-1}$ under a scenario of reducing oxygen availability, shoals will have to become either smaller or less

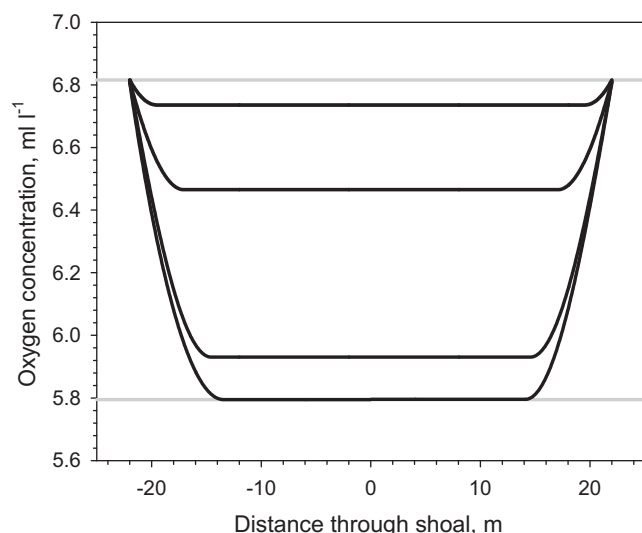


Figure 3. Modeled Oxygen Concentration by Distance through a Krill Shoal
Variation in oxygen concentration by distance through a krill shoal (containing animals of length = 45.4 mm, swimming at a nominal speed of 20 cm/s) with diameter set to the mean of all x, y, and z shoal dimensions (0 m is the shoal center) and median packing density (111 krill per m³). Curves are, from top to bottom, time = 50 s, 100 s, 150 s, and 159 s. The upper horizontal gray line indicates the ambient oxygen concentration, and the lower horizontal gray line marks the critical oxygen threshold for krill [39]. Note that at any time, oxygen concentration effectively takes either one of just two possible values: a low value inside the shoal where respiratory consumption dominates, or a high value at the shoal edge where diffusive replacement dominates.

densely packed. Community schooling behavior is known to be impacted by fluctuating oxygen minima [34], and changing oxygen concentration may disrupt predator-prey interactions [38]. Furthermore, the ease (or difficulty) with which fishermen can catch pelagic fish and crustaceans—catchability—can vary as a function of shoal size [13], so understanding the response of shoals to changing oxygen concentration will be of commercial as well as ecological importance.

Supplemental Information

Supplemental Information includes three figures, two tables, and Supplemental Experimental Procedures and can be found with this article online at doi:10.1016/j.cub.2010.08.041.

Acknowledgments

M.J.C. was funded by a PhD studentship from the UK Natural Environment Research Council, with additional support from the Russell Trust. Antarctic fieldwork was carried out in conjunction with D.A. Demer and J.D. Warren under their US National Science Foundation grant 06-OPP-33939, with equipment support from the UK Royal Society and logistic support from the US Antarctic Marine Living Resources program; we thank R.S. Holt for access to that program's facilities. We thank J. Condiotty, Simrad USA, for loan of the multibeam sonar, and S. Sessions, A. Jenkins, D. Needham, the crew of the RV *Yuzhmorgeologiya*, and personnel at the Cape Shirreff field camp for assistance in the field. A.S.B. acknowledges travel support from the Royal Society and the Australian National Network in Marine Science that enabled him to discuss aspects of this work with Australian experts at a key phase in the revision of this manuscript.

Received: August 21, 2009

Revised: July 12, 2010

Accepted: August 19, 2010

Published online: September 16, 2010

References

- Krause, J., and Ruxton, G.D. (2002). *Living in Groups* (Oxford: Oxford University Press).
- Ballerini, M., Cabibbo, N., Candelier, R., Cavagna, A., Cisbani, E., Giardina, I., Orlandi, A., Parisi, G., Procaccini, A., Viale, M., and Zdravkovic, V. (2008). Empirical investigation of starling flocks: A benchmark study in collective animal behaviour. *Anim. Behav.* 76, 201–215.
- Ballerini, M., Cabibbo, N., Candelier, R., Cavagna, A., Cisbani, E., Giardina, I., Lecomte, V., Orlandi, A., Parisi, G., Procaccini, A., et al. (2008). Interaction ruling animal collective behavior depends on topological rather than metric distance: Evidence from a field study. *Proc. Natl. Acad. Sci. USA* 105, 1232–1237.
- Cox, M.J., Warren, J.D., Demer, D.A., Cutter, G.R., and Brierley, A.S. (2010). Three-dimensional observations of swarms of Antarctic krill (*Euphausia superba*) made using a multi-beam echosounder. *Deep Sea Res. II Top. Stud. Oceanogr.* 57, 508–518.
- Cox, M.J., Demer, D.A., Warren, J.D., Cutter, G.R., and Brierley, A.S. (2009). Multibeam echosounder observations reveal interactions between Antarctic krill and air-breathing predators. *Mar. Ecol. Prog. Ser.* 378, 199–209.
- Gerlotto, F., Castillo, J., Saavedra, A., Barbieri, M.A., Espejo, M., and Cotel, P. (2004). Three-dimensional structure and avoidance behaviour of anchovy and common sardine schools in central southern Chile. *ICES J. Mar. Sci.* 61, 1120–1126.
- Gerlotto, F., and Paramo, J. (2003). The three-dimensional morphology and internal structure of clupeid schools as observed using vertical scanning multibeam sonar. *Aquat. Living Resour.* 16, 113–122.
- Paramo, J., Bertrand, S., Villalobos, H., and Gerlotto, F. (2007). A three-dimensional approach to school typology using vertical scanning multibeam sonar. *Fish. Res.* 84, 171–179.
- Parrish, J.K., and Edelstein-Keshet, L. (1999). Complexity, pattern, and evolutionary trade-offs in animal aggregation. *Science* 284, 99–101.
- Garcia, H.E., Boyer, T.P., Levitus, S., Locarnini, R.A., and Antonov, J. (2005). On the variability of dissolved oxygen and apparent oxygen utilization content for the upper world ocean: 1955 to 1998. *Geophys. Res. Lett.* 32, L09604.
- Fréon, P., and Misund, O.A. (1999). *Dynamics of Pelagic Fish Distribution and Behaviour: Effects on Fisheries and Stock Assessment* (Oxford: Fishing News Books, Blackwell Science Ltd.).
- Mori, Y., and Boyd, I.L. (2004). The behavioral basis for nonlinear functional responses and optimal foraging in Antarctic fur seals. *Ecology* 85, 398–410.
- Zhou, S.J., Dichmont, C., Burrige, C.Y., Venables, W.N., Toscas, P.J., and Vance, D. (2007). Is catchability density-dependent for schooling prawns? *Fish. Res.* 85, 23–36.
- Pitcher, T.J. (1983). Heuristic definitions of fish shoaling behavior. *Anim. Behav.* 31, 611–613.
- Hamner, W.M., and Hamner, P.P. (2000). Behavior of Antarctic krill (*Euphausia superba*): Schooling, foraging, and antipredatory behavior. *Can. J. Fish. Aquat. Sci.* 57, 192–202.
- Miller, D.G.M., and Hampton, I. (1989). *Biology and Ecology of the Antarctic Krill (Euphausia superba Dana): A Review*, BIOMASS Scientific Series, Volume 9 (Cambridge: SCAR and SCOR).
- Blaxter, J.H.S., and Hunter, J.R. (1982). The biology of Clupeoid fishes. *Adv. Mar. Biol.* 20, 1–223.
- Watkins, J.L., and Murray, A.W.A. (1998). Layers of Antarctic krill, *Euphausia superba*: Are they just long krill swarms? *Mar. Biol.* 131, 237–247.
- Holliday, D.V., Donaghay, P.L., Greenlaw, C.F., Napp, J.M., and Sullivan, J.M. (2009). High-frequency acoustics and bio-optics in ecosystems research. *ICES J. Mar. Sci.* 66, 974–980.
- Bertrand, A., Gerlotto, F., Bertrand, S., Gutierrez, M., Alza, L., Chipollini, A., Diaz, E., Espinoza, P., Ledesma, J., Quesquen, R., et al. (2008). Schooling behaviour and environmental forcing in relation to anchoveta distribution: An analysis across multiple spatial scales. *Prog. Oceanogr.* 79, 264–277.
- Hamilton, W.D. (1971). Geometry for the selfish herd. *J. Theor. Biol.* 31, 295–311.
- Axelsen, B.E., Anker-Nilssen, T., Fossum, P., Kvamme, C., and Nottestad, L. (2001). Pretty patterns but a simple strategy: Predator-prey interactions between juvenile herring and Atlantic puffins observed with multibeam sonar. *Can. J. Zool.* 79, 1586–1596.

23. Gerlotto, F., Soria, M., and Freon, P. (1999). From two dimensions to three: The use of multibeam sonar for a new approach in fisheries acoustics. *Can. J. Fish. Aquat. Sci.* **56**, 6–12.
24. Parrish, J.K. (1989). Reexamining the selfish herd: Are central fish safer? *Anim. Behav.* **38**, 1048–1053.
25. Laws, R.M. (1985). The ecology of the Southern Ocean. *Am. Sci.* **73**, 26–40.
26. Woods, H.A., and Moran, A.L. (2008). Oxygen profiles in egg masses predicted from a diffusion-reaction model. *J. Exp. Biol.* **211**, 790–797.
27. McFarland, W.N., and Moss, S.A. (1967). Internal behavior in fish schools. *Science* **156**, 260–262.
28. Johnson, M.A., Macaulay, M.C., and Biggs, D.C. (1984). Respiration and excretion within a mass aggregation of *Euphausia superba*: Implications for krill distribution. *J. Crustacean Biol.* **4**, 174–184.
29. Strand, S.W., and Hamner, W.M. (1990). Schooling behaviour of Antarctic krill (*Euphausia superba*) in laboratory aquaria: Reactions to chemical and visual stimuli. *Mar. Biol.* **106**, 355–359.
30. Domenici, P., Steffensen, J.F., and Batty, R.S. (2000). The effect of progressive hypoxia on swimming activity and schooling in Atlantic herring. *J. Fish Biol.* **57**, 1526–1538.
31. Moss, S.A., and McFarland, W.N. (1970). Influence of dissolved oxygen and carbon dioxide on fish schooling behaviour. *Mar. Biol.* **5**, 100–107.
32. Domenici, P., Lefrançois, C., and Shingles, A. (2007). Hypoxia and the antipredator behaviours of fishes. *Philos. Trans. R. Soc. Lond. B Biol. Sci.* **362**, 2105–2121.
33. Kramer, D.L. (1987). Dissolved oxygen and fish behaviour. *Environ. Biol. Fishes* **18**, 81–92.
34. Bertrand, A., Barbieri, M.A., Gerlotto, F., Leiva, F., and Cordova, J. (2006). Determinism and plasticity of fish schooling behaviour as exemplified by the South Pacific jack mackerel *Trachurus murphyi*. *Mar. Ecol. Prog. Ser.* **311**, 145–156.
35. Gueron, S., Levin, S.A., and Rubenstein, D.I. (1996). The dynamics of herds: From individuals to aggregations. *J. Theor. Biol.* **182**, 85–98.
36. Tien, J.H., Levin, S.A., and Rubenstein, D.I. (2004). Dynamics of fish shoals: Identifying key decision rules. *Evol. Ecol. Res.* **6**, 555–565.
37. Guillard, J., Brehmer, P., Colon, M., and Guennegan, Y. (2006). Three dimensional characteristics of young-of-year pelagic fish schools in lake. *Aquat. Living Resour.* **19**, 115–122.
38. Abrahams, M.V., Mangel, M., and Hedges, K. (2007). Predator-prey interactions and changing environments: Who benefits? *Philos. Trans. R. Soc. Lond. B Biol. Sci.* **362**, 2095–2104.
39. Kils, U. (1979). Performance of Antarctic krill *Euphausia superba*, at different levels of oxygen saturation. *Meeresforschung* **27**, 35–48.